NASA CR-121157
AI-73-31

FINAL REPORT

S8DR SHIELD EXAMINATION

by

D. G. Mason and W. R. McCurnin

ATOMICS INTERNATIONAL DIVISION
ROCKWELL INTERNATIONAL CORPORATION

prepared for

NATIONAL AERONAUTICS AND SPACE ADMINISTRATION

NASA Lewis Research Center
Contract NAS 3-15705
L. Kaszubinski, Project Manager

NOTICE

This report was prepared as an account of Government-sponsored work. Neither the United States, nor the National Aeronautics and Space Administration (NASA), nor any person acting on behalf of NASA:

A.) Makes any warranty or representation, expressed or implied, with respect to the accuracy, completeness, or usefulness of the information contained in this report, or that the use of any information, apparatus, method, or process disclosed in this report may not infringe privately owned rights; or

B.) Assumes any liabilities with respect to the use of, or for damages resulting from the use of any information, apparatus, method or process disclosed in this report.

As used above, "person acting on behalf of NASA" includes any employee or contractor of NASA, or employee of such contractor, to the extent that such employee or contractor of NASA, or employee of such contractor prepares, disseminates, or provides access to, any information pursuant to his employment or contract with NASA, or his employment with such contractor.

Request for copies of this report should be referred to:

National Aeronautics and Space Administration
Scientific and Technical Information Facility
P.O. Box 33
College Park, Md. 20740

1. Report No.	2. Government Accession No.	3. Recipient's Catalog No.
NASA-CR-121157		

4. Title and Subtitle	5. Report Date
S8DR SHIELD EXAMINATION	January 1973
	6. Performing Organization Code

7. Author(s)	8. Performing Organization Report No.
D. G. Mason and W. R. McCurnin	AI-73-31
	10. Work Unit No.

9. Performing Organization Name and Address	11. Contract or Grant No.
Atomics International Canoga Park, California	NAS 3-15705
	13. Type of Report and Period Covered
12. Sponsoring Agency Name and Address	Contractor Report
National Aeronautics and Space Administration Cleveland, Ohio 44135	14. Sponsoring Agency Code

15. Supplementary Notes

Project Manager, Leonard J. Kaszubinski, NASA Lewis Research Center, Cleveland, Ohio

16. Abstract

The SNAP 8 Developmental Reactor (S8DR) lithium hydride (LiH) shield was examined after being irradiated for over 7000 hours at relatively low temperature. A crack was located in the seam weld of the containment vessel, probably the result of hot short cracking under thermal stress. The LiH was visually examined at two locations and its appearance was typical of low temperature irradiated LiH. The adherence of the chrome oxide emittance coating was found to be excellent.

17. Key Words (Suggested by Author(s))	18. Distribution Statement
SNAP shielding Lithium hydride S8DR	Unclassified - unlimited

19. Security Classif. (of this report)	20. Security Classif. (of this page)	21. No. of Pages	22. Price*
Unclassified	Unclassified	54	$3.00

* For sale by the National Technical Information Service, Springfield, Virginia 22151

Page Intentionally Left Blank

NASA CR-121157
AI-73-31

FINAL REPORT

S8DR SHIELD EXAMINATION

by

D. G. Mason and W. R. McCurnin

ATOMICS INTERNATIONAL DIVISION
ROCKWELL INTERNATIONAL CORPORATION
8900 De Soto Avenue
Canoga Park, California 91304

prepared for

NATIONAL AERONAUTICS AND SPACE ADMINISTRATION

January 1973

CONTRACT NAS 3-15705

NASA Lewis Research Center
Cleveland, Ohio
L. Kaszubinski, Project Manager

Page Intentionally Left Blank

CONTENTS

		Page
Abstract		vii
I.	Summary	1
II.	Introduction	2
III.	Discussion of Test Results	3
	A. Phase A	3
	1. Visual Examination	3
	2. Gas Analysis	3
	3. Adherence Testing	5
	4. Leak Testing	5
	B. Phase B	6
	1. Confinement Vessel Removal	6
	2. Leak Testing	7
	C. Phase C	7
	1. Crack Examination	7
	2. LiH Examination	10
IV.	Summary of Results	10
Appendix A – S8DR Shield Examination		29

FIGURES

1.	DR106. Lithium Hydride Shield as received, at 0°	12
2.	Gas Sampling Schematic	13
3A.	DR110. Area near top of shield before application of Tucktape	14
3B.	DR111. Area near top of shield after application of Tucktape. No oxide adhered to the tape, only surface dust.	14
3C.	DR112. Area near top of shield after 12 rubbing strokes with 180 grit paper	14
3D.	DR114. Area near top of shield after the scribing attempt. The chromic oxide material remained on the shield.	14
4A.	DR115. Area 6" from bottom of shield before application of Tucktape.	15
4B.	DR116. Area 6" from bottom of shield after application of Tucktape. No oxide adhered to the tape, only surface dust.	15

FIGURES

Page

4C. DR117. Area 6" from bottom of shield after 72 rubbing strokes with 180 grit paper. 15

4D. DR118. Area 6" from bottom of shield after using the scribing tool. 15

5. DR-121. Shield after confinement vessel removal, at 180° 16

6. DR-128. Bulge determination using a straight edge across top of shield. 17

7A. DR-126. Small crack in side wall of shield ~1/4" long, 4" below top weld at 270°. 18

7B. DR-127. Low power Kollmorgen shot showing orientation of small crack. 18

8. DR-134. Stainless Steel Wafter – Back side showing weld bead – main crack is centrally located (1.3X) 19

9. DR-132. Closeup (3.4X) of Main Crack in Weld. 19

10. DR-133. Typical Crystalline Strcuture of Irradiated LiH (1.4X). . . . 20

11. DR-141. X-ray Showing Crack (taken perpendicular to face of wafer). 20

12. DR-152. X-ray Taken 45 Degrees to Face of Wafer. 21

13. DR-141. Photograph of Main Crack – Inside Surface (12.8X). 22

14. DR-147. Photograph of Hairline Crack Located ~1/2 inch From Main Crack (12.8X) 22

15. DR-142. Photograph of Three Small Cracks Located ~1/4 inch from Main Crack (12.8X). 23

16. Stereo Photograph of Weld Showing Cracks (12.8X). 24

17. DR-148. Stereo Photograph of Outside Surface Showing Main Crack and Other Surface Cracks Not Related to Other Metal Cracks (12.8X). 25

18. DR-149. Stereo Photograph of Outside Surface Showing Emissivity Coating Cracks Not Related to Metal Cracks (4.3X). 25

19. DR-130. Pipe Elbow Showing Lithium Hydroxide in Pipe Nipple. . . . 26

20. DR-140. View of Wafer Cut Out of Top Head Showing Inside Surface (1.4X). 26

21. DR-139. View of Wafer Cut From Center of Head Showing LiH Crystalline Structure at Shield End of Pipe Nipple (1.4X). 27

22. DR-136. View of Wafer and Hole at Shield Head Mid-radius 27

ABSTRACT

The SNAP 8 Developmental Reactor (S8DR) lithium hydride (LiH) shield was examined after being irradiated for over 7000 hours at relatively low temperature. A crack was located in the seam weld of the containment vessel, probably the result of hot short cracking under thermal stress. The LiH was visually examined at two locations and its appearance was typical of low temperature irradiated LiH. The adherence of the chrome oxide emittance coating was found to be excellent.

I. SUMMARY

The gas in the confinement space was sampled and it was determined that there was < 25 ppm water and < 2% oxygen in the space. The adherence of the chrome oxide coating was determined to be good based on tests at the top of the confinement vessel and approximately 6 inches from the bottom. The testing consisted of application of 2 inch squares of Tacktape, rubbing selected areas with 180 grit emery paper and attempting to scrape with a scribing tool. The shield was leak tested while in the confinement vessel and determined to have a leak rate calculated to be > 1.2 cc/sec.

The confinement vessel was then removed from the shield using a cutting torch. The shield was pressurized to approximately 25 psia helium and leak tested using a helium sniffing probe. A small crack approximately 1/4 inch long, 4 inches below the top weld was located. After this crack was located it was sealed and the remainder of the shield leak tested using the sniffing probe and found to have no leaks $> 3.8 \times 10^{-6}$ cc/sec. A bulge was noted over the top surface of the shield. This bulge was estimated to be 5/8 inch.

A 2 inch diameter hole saw was used to remove the crack area, an area located elsewhere in the weld, at the top center of the shield (bulge area) and at the mid-radius location on the top of the shield. The lithium hydride beneath all the samples removed was black crystalline in nature and appeared typical of low temperature irradiated LiH. The fill pipe at the top center of the shield contained a white crystalline substance which was apparently lithium hydroxide. Visual examination of the main crack area on the inside portion of the sample indicated several smaller apparent cracks which had not penetrated the thickness of the cladding. X-ray examination of the main crack revealed that it penetrated the thickness of the clad and extended the full width of the weld with the crack plane at a 45° angle to the plane of the base metal. None of the smaller apparent cracks and no inclusions were visible in the X-rays, nor were the smaller apparent cracks shown by dye-penetrant inspection indicating little depth to the apparent cracks.

The metallurgical examination showed little effects of planishing and did not show any appreciable amount of ferrite in the weld zone. Both of these indicated very little weld filler rod was used in the weld. Literature data indicates that good thermal cycle weld stability in 347 stainless steel is attained by controlling the ferrite concentration used in the weld filler rods. Thus, it is not surprising that the weld failed, probably during shutdown, as the examination showed the LiH to have swelled causing a differential thermal contraction which stressed the weld zone and resulted in the shear fracture observed.

II. INTRODUCTION

The main purpose of this contract was to determine if the S8DR shield containment had been breached during operations as indicated by the operations data at shutdown of the S8DR, and if so, what was the cause of the failure. To establish this a three phase contract, with each phase being separately negotiated, was undertaken by AI for the NASA-Lewis Research Center. The three phase program was to determine, (A) if a leak truly existed, (B) the exact location of the leak or leaks, and (C) the cause of the leak. These three tasks were conducted in the three separate phases of the contract.

Phase A consisted of determining if there was a leak between the shield container and the confinement vessel by helium leak checking techniques. In addition the adherence of the high emittance chrome oxide coating on the confinement vessel was evaluated and the gas between the shield and the confinement vessel was also analyzed to assure that no gross leakage of air into this space had occurred which could invalidate any LiH examination.

Phase B consisted of locating the leak found in Phase A. This resulted in the removal of the confinement vessel and a detailed visual examination of the shield.

Phase C consisted of a detailed metallurgical examination of a crack located during Phase B. Concurrent with the crack examination, a limited inspection of the LiH in selected areas was also conducted.

III. DISCUSSION OF TEST RESULTS

A. PHASE A

1. Visual Examination

The shield was shipped from the Radioactive Materials Disposal Facility (RMDF) to the Atomics International Hot Laboratory (AIHL) and unloaded into Cell #4 on April 10, 1972. Photographs were taken of the shield as received on four orientations through the cell window. The appearance of the shield was excellent (Figure 1).

2. Gas Analysis

The gas contained in the confinement space between the shield and the confinement vessel was sampled. Refer to the schematic (Figure 2) for the following description of the gas sampling. A 1/4 inch hole was drilled through the aluminum cap cover on the 4.5 inch pipe. A hypodermic needle attached to two gas sample containers was pushed about 1/4 inch into the rubber cap gasket so the hole in the needle would be sealed. The sample containers and line to the needle were evacuated to less than 1 micron. The sample containers were isolated from the vacuum

pump by closing valve #4 and sample container #2 by shutting off valve #3. The needle was pushed through the rubber gasket noting the drop in vacuum to zero inches of vacuum. The inlet valve (#1) to sample container #1 was closed and inlet valve (#3) to sample container #2 was opened. Vacuum on both containers now read 26 inches of vacuum. The inlet valve (#1) to sample container #1 was opened allowing gas to flow through container #1 into container #2. Valves #1, #2 and #3 were left open for 2 minutes to allow complete filling of sample containers. All valves were closed, the needle removed from the shield, the sample containers disconnected and capped for shipment.

Sample container #2 was sent to Health Physics to determine the concentration of tritium in the gas. It was determined by analysis that the concentration was 2.6×10^{-2} μci/cc. This allowed for an exempt shipment to an outside vendor for analysis. The gas was analyzed by standard mass spectrographic analysis for gases. Individual standard gases were analyzed to determine sensitivity.

The results of the gas analysis are shown in Table I.

TABLE I

Constituent	Mole Percent
Hydrogen	2.27 ± .01
Helium	9.15 ± .01
Nitrogen	27.32 ± .01
Argon	59.34 ± .01
Oxygen	1.92 ± .01
Water	23 ppm ± 2 ppm

3. Adherence Testing

The adherence of the chromic oxide coating was tested at the top of the confinement vessel and approximately 6 inches from the bottom of the confinement vessel.

The testing consisted of application of 2 inch squares of Tucktape, rubbing selected areas with 180 grit emery paper and attempting to scrape with a scribing tool. Photographs were taken of the shield area before and after the above operations.

Figure 3 shows the area near the top of the shield before application of the Tucktape (3A), after application of the tape (3B), after 12 rubbing strokes with 180 grit paper (3C), and after the scribing attempt (3D). The Tucktape did not remove any chromic oxide material. The material removed as indicated in the photograph was essentially surface dust. The external appearance in the rubbed area changed from gray to light green after 12 rubbing strokes with the 180 grit paper. There was no further change after 24 strokes or 72 strokes. It was not possible to penetrate to base metal with a scribe tool in this area.

Figure 4 shows an area 6 inches from the bottom of the shield before application of the Tucktape (4A), after application of the Tucktape (4B), after 72 strokes using 180 grit paper (4C) and after using the scribing tool (4D). There was no chromic oxide coating removed using the Tucktape. The material removed as indicated in 4B is surface dust. After 72 strokes with the 180 grit paper, bare metal was just showing through. It was not possible to scrape through to bare metal with the scribing tool.

4. Leak Testing

The 4 inch pipe was cut off from the shield by using a hacksaw on the straight portion and a tubing cutter 1 inch from the top of the shield.

The 3/4 inch pipe inside the 4 inch pipe was cut off using a remote hacksaw. The space between the shield and confinement vessel was purged with dry nitrogen for 40 hours at 25 cu ft/min. A plug was made to place in the 4 inch pipe. The space between the shield and confinement vessel was evacuated for two days. A tube connected to the 3/4 inch pipe was hooked to a vacuum gauge at the end of two day. The gauge showed 26 inches of vacuum indicating a leak from the shield into the confinement space. The helium leak indicator indicated a background on the confinement vessel space of 0.76×10^{-6} cc/sec. An attempt was made to put one atmosphere of helium into the shield. The leak detector went immediately off scale at 7.2×10^{-6} cc/sec. A known volume of helium, 1457 cc, was pressurized to 284 psi. The quantity of gas in this vessel was then calculated to allow one atmosphere of helium pressure in the void volume of the shield. The helium gas was bled into the shield over a 6 hour 23 minute time period by throttling the pressure into the shield to 15 psi or less. After the standard volume pressure decreased to 15 psi the shield pressure decreased to zero psi in 8 minutes. It was assumed that the gas was leaking nearly as rapidly as it was being admitted. On this basis the leak rate was calculated to be > 1.2 cc/sec.

B. PHASE B

1. Confinement Vessel Removal

A cutting torch was used to remove the support brackets and confinement vessel. The confinement vessel was removed by cutting circumferentially 1 inch below the weld joining the conical section to the cylindrical section. A sling was used to lift the confinement vessel off the shield. Photographs were taken of the shield on four orientations through the cell window. Figure 5 shows the overall condition of the shield at 180°. The shield appeared very clean. Some small areas of apparently

spalling emissivity were noted where the top head and side meet. Otherwise no surface anomalies were noted. A straight edge was placed across the top of the shield to determine if any bulging was present. A bulge of 5/8 inch was estimated as shown in Figure 6. A straight edge was also placed along the side wall near the crack. No bulge could be determined when compared to several other areas on the shield.

2. Leak Testing

The shield was pressurized to approximately 25 psia helium using the 3/4 inch pipe. The shield was then examined for leaks using a helium sniffing probe. A small crack, ~ 1/4 inch long, 4 inches below the top weld, was located. Figure 7 shows the crack and crack location. The remainder of the shield was then leak tested.

A standard leak was used to calibrate a CEC 120 type Leak Detector. The vacuum method of calibration was used. The sensitivity achieved was 1.7×10^{-10} cc/sec/unit. As stated in the leak detector manufacturers instructions, the probe method of testing is 1/100 the sensitivity of vacuum testing at best. Due to the length of hose and in-cell conditions the sensitivity is estimated to be 1/1000 of vacuum testing. Using the manufacturers instructions a sensitivity of 1.7×10^{-8} cc/sec/unit was achieved. No leaks greater than 3.8×10^{-6} cc/sec other than the crack in the side wall, were detected using the 1.7×10^{-8} cc/sec/unit sensitivity.

C. PHASE C

1. Crack Examination

A two inch diameter wafer containing the crack was cut away under an argon purge from the shield side using a hole saw. The wafer (Figure 8) was readily removed. Visual examination of the back side

(side next to LiH) showed the crack clearly (Figure 9) and that it was on the weld seam as suspected. The LiH exposed when the wafer was removed had the characteristic appearance of irradiated LiH. Figure 10 shows the black, crystalline structure exposed after chipping out a sample. The sample was stored in a polyethylene bottle under an argon gas. The hole in the shield container was then sealed with epoxy and the argon purge terminated.

The wafer was removed from the cell and X-rayed perpendicular to the wafer and at a 45 degree angle (Figures 11 and 12 respectively). The X-rays clearly show the crack plane to be at a 45 degree angle to the plane of the base metal. No inclusions or other cracks are visible in the X-rays.

A stereomicroscopic (12.8x) examination of the wafer revealed additional surface "cracks" in the vicinity of the main crack (Figure 13). Figure 14 shows a hairline "crack" about 1/4 inch from the main crack. Figure 15 shows three small "cracks" located about 3/4 inch from the main crack. All the small "cracks" run essentially parallel to the main crack. The emissivity coating prevents identifying any crack from the outside except for the main crack which obviously penetrated. Figure 16 is a composite photograph taken at 4.3X across the wafer showing the complete weld bead. Figures 17 and 18 show the outside surface of the wafer. The entire weld bead was dye-penetrant inspected to determine if any other cracks existed. Only the main crack was identified indicating that the smaller "cracks" had very little depth. Subsequent metallographic examination removed all indications in polishing the surface confirming that the smaller "cracks" were just surface flaws a similar one of which could have been the initiation flaw for the main crack.

Based on the visual metallurgical examination of the weld the crack extended transverse to the weld fusion zone and slightly into the heat effected zone on both sides of the fusion zone, Figure 1, Appendix A. The crack extended through the weld. It was noted that the I. D. (root side) had not been made fully flush by the roll planishing operation as evidenced by 0.005 - 0.010 inch protrusion of residual dropthrough (Figure 2, Appendix A). The section was mounted such that the face surface (Figure 2, Appendix A) was accessible for polishing. This surface was prepared metallographically for analysis of the microstructure.

Examination of the metallographic mount showed that the crack was intergranular and appeared to initiate at a small discontinuity at the approximate center of the weld (Figures 3 and 4, Appendix A). It was also noted that the dendritic structure was distorted, apparently a result of planishing, and did not follow a normal semi-circular or triangular freezing pattern (Figures 1 and 3, Appendix A). There were islands of what initially appeared as equiaxed grain structure observed in the fusion zone (Figures 1, 3, and 4, Appendix A). This was considered abnormal for the weld involved and was later interpreted as recrystallized cold-worked material (see discussion in Appendix A). The structure was essentially all-austenitic with virtually no delta ferrite visible (Figure 4, Appendix A). This conclusion was reached by comparing the viewed structures with weld structures known to contain specific delta ferrite contents. The dendritic formations (other than being distorted) were generally long, narrow, and almost perpendicular to the direction of rolling (Figures 1 and 3, Appendix A). There was no evidence of sigma phase.

A complete discussion of the fabrication process and the metallurgical examination of the weld and crack is contained in Appendix A.

2. LiH Examination

The pipe nipple elbow was first cut off (Figure 19) in preparation for a hole saw cut in the center of the top. The lithium hydride in this area has apparently changed to lithium hydroxide. As this area had been exposed to normal cell atmosphere for over two months, it is not surprising to find lithium hydroxide here. A sample of the material was taken and placed in a polyethylene bottle under argon.

A purge of argon was started and the center pipe was cut out with the hole saw (Figures 20 and 21). The pipe appears to be filled with lithium hydroxide while the material in the shield can has the typical appearance of irradiated LiH, i.e., a black, crystalline appearance. A hole was also cut at half-radius (Figure 22). The LiH here also appears typical of irradiated LiH. Samples were taken from both locations and sealed under argon. The LiH at both locations appear to be tight against the stainless steel container. Both holes were sealed with epoxy after the LiH samples were taken.

A sample of LiH was also taken under the wafer removed for the crack examination. The LiH here was also crystalline in nature and typical of low temperature irradiation.

IV. SUMMARY OF RESULTS

A large leak was determined to exist as a result of leak testing during Phase A. Upon removal of the confinement vessel, a crack about 3/4 inch long was located in the seam weld of the shield vessel approximately 4 inches from the top. Metallurgical examination of this crack showed it to be a shear type failure. A detailed metallurgical examination was conducted and the results of this examination concluded that the crack probably emanate from a weld fissure or similar weakness which was not detected during original fabrication; for example, the

surface flaws observed visually but lacking sufficient depth to be detected by a dye-penetrant examination. Such fissures are not uncommon to type 347 stainless steel and can usually be prevented by adding weld filler metal containing small amounts of delta ferrite material. The metallography in the vicinity of the crack indicated little if any weld filler metal was added.

The chrome oxide emittance coating was in excellent condition on both the confinement vessel and the shield vessel.

The LiH observed in selected regions appeared to be dull black and crystalline in nature, typical of that expected when irradiated at low temperature. Some growth was evidenced by bulging of the top of the shield container. This radiation growth is not unexpected considering the low temperature operation of the shield. The growth, however, probably contributed to the stress level in the weld area.

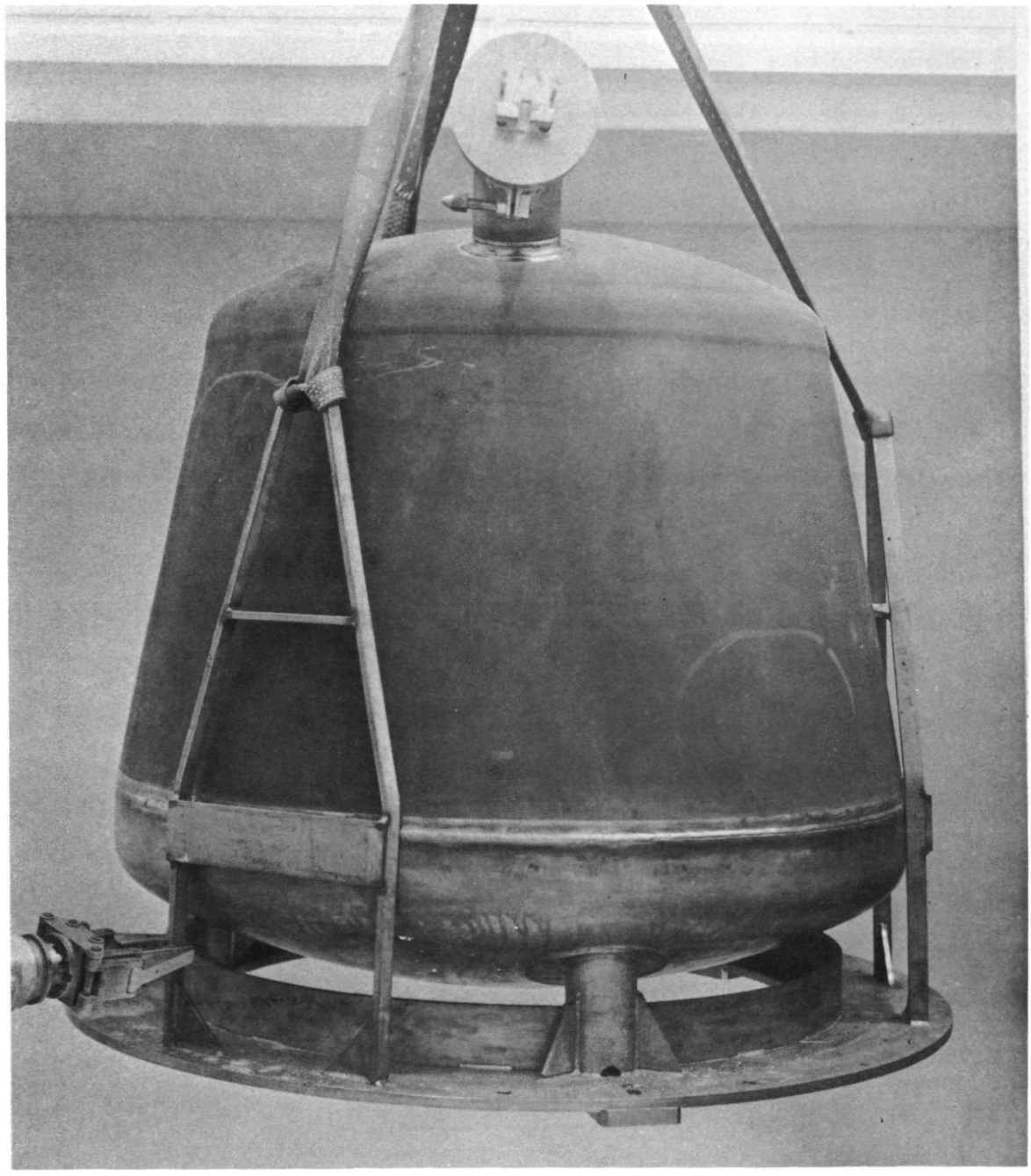

Figure 1 - DR106. Lithium Hydride Shield as received, at 0°.

Figure 2

GAS SAMPLING SCHEMATIC

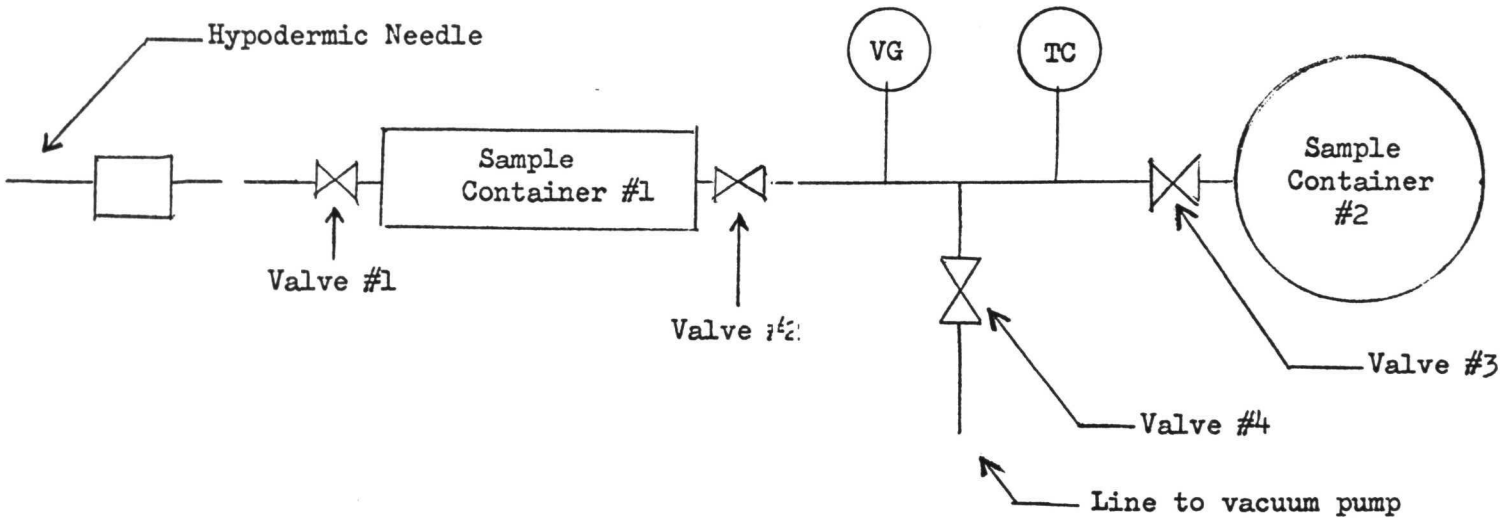

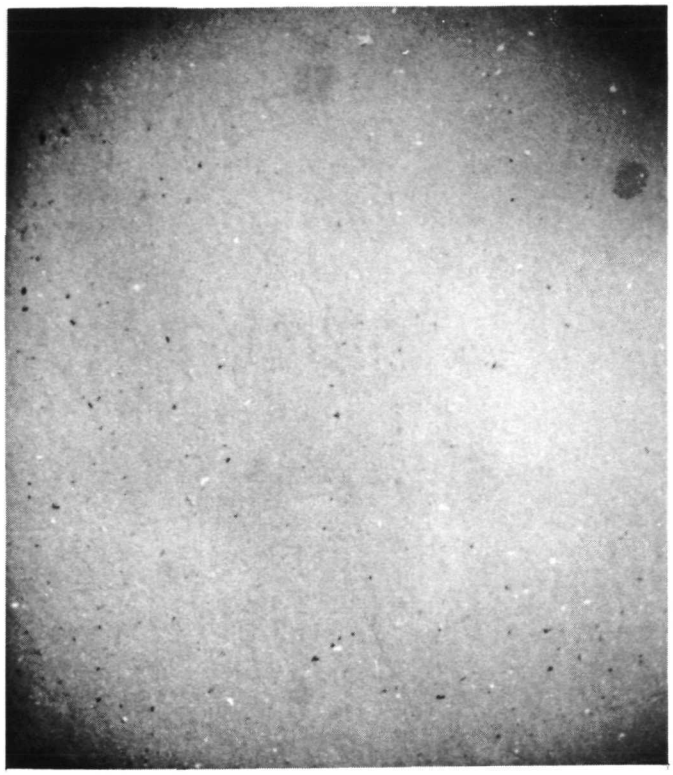

Figure 3A - DR110. Area near top of shield before application of Tucktape.

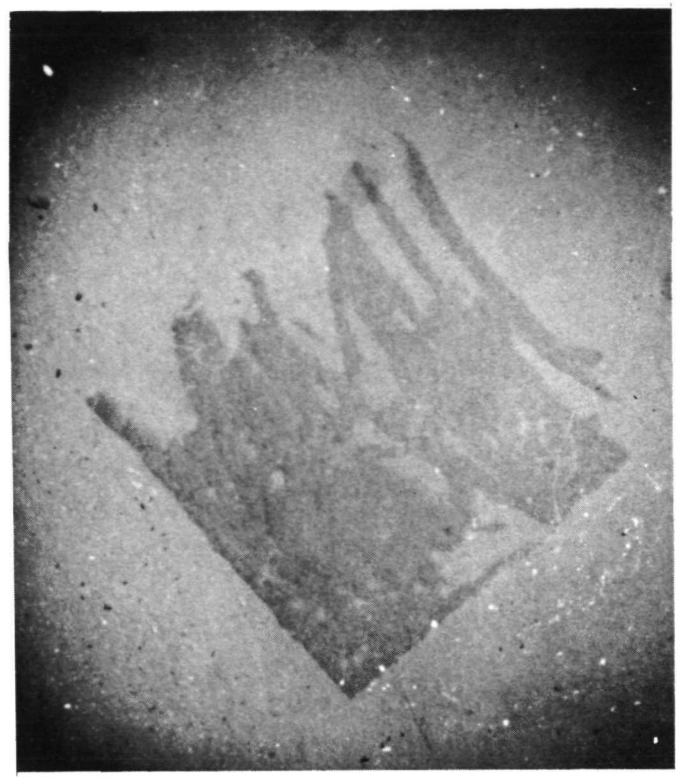

Figure 3B - DR111. Area near top of shield after application of Tucktape. No oxide adhered to the tape, only surface dust.

Figure 3C - DR112. Area near top of shield after 12 rubbing strokes with 180 grit paper.

Figure 3D - DR114. Area near top of shield after the scribing attempt. The chromic oxide material remained on the shield.

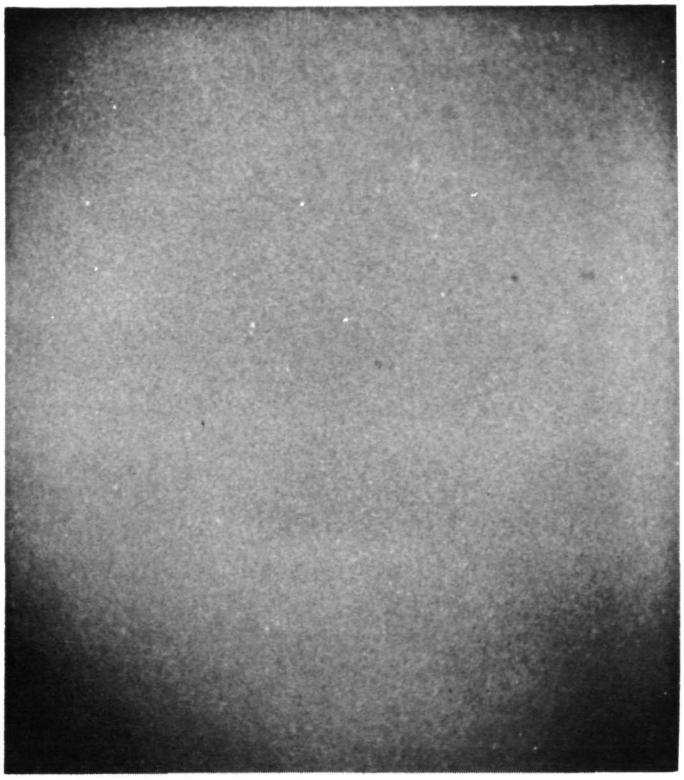

Figure 4A - DR115. Area 6" from bottom of shield before application of Tucktape.

Figure 4B - DR116. Area 6" from bottom of shield after application of Tucktape. No oxide adhered to the tape, only surface dust.

Figure 4C - DR117. Area 6" from bottom of shield after 72 rubbing strokes with 180 grit paper.

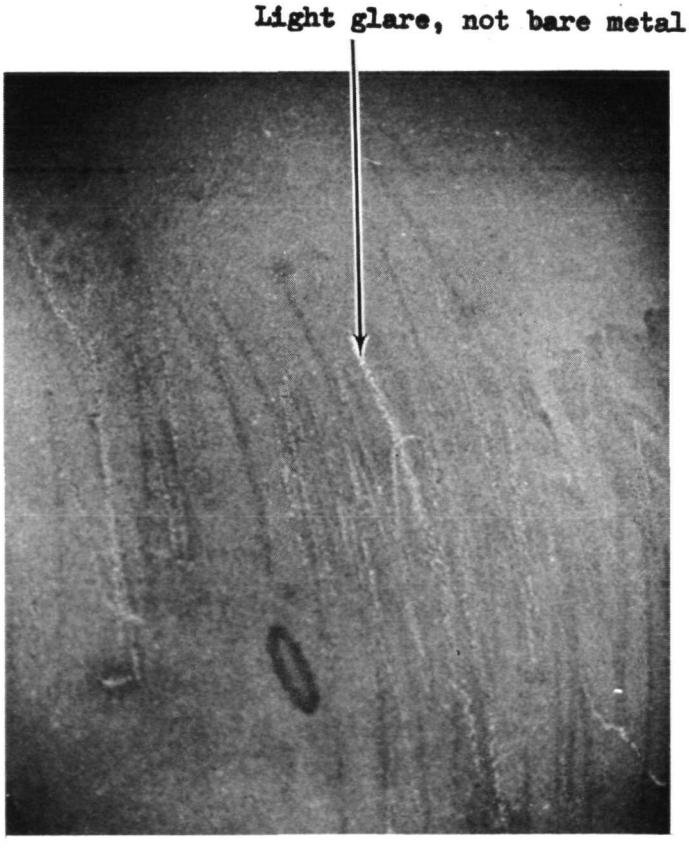

Figure 4D - DR118. Area 6" from bottom of shield after using the scribing tool.

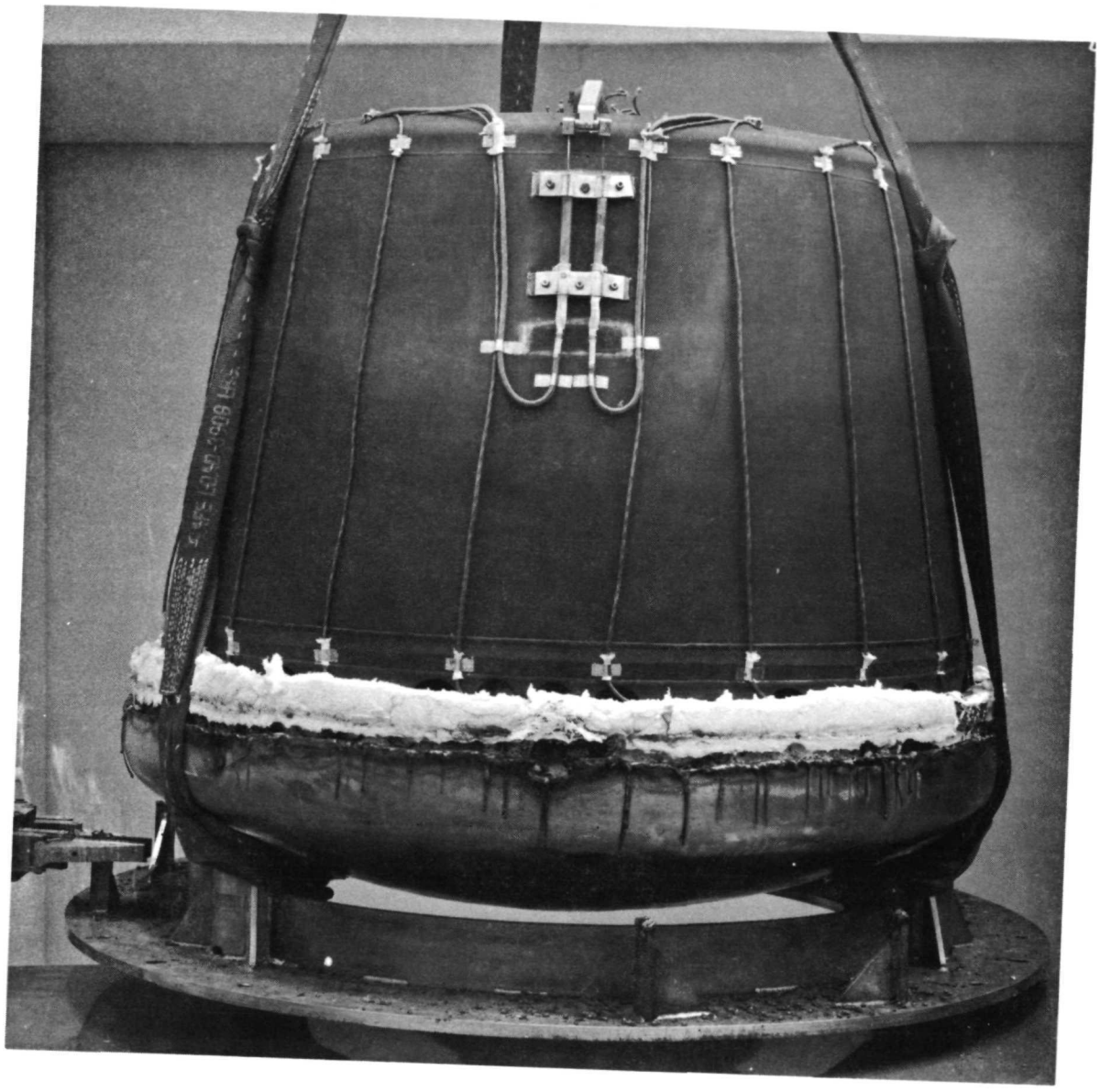

Figure 5, DR-121. Shield after confinement vessel removal, at 180°.

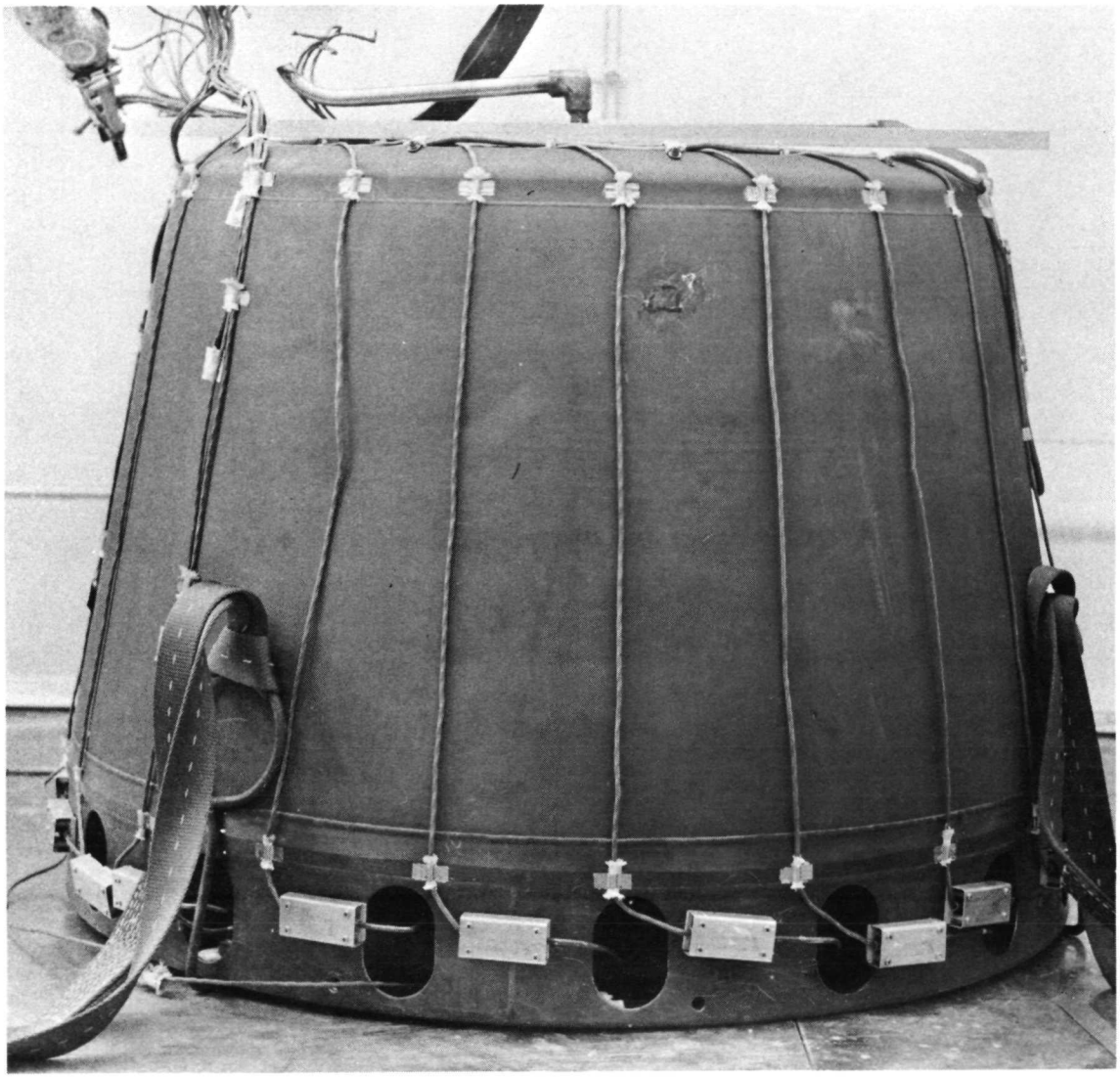

Figure 6, DR-128. Bulge determination using a straight edge across top of shield.

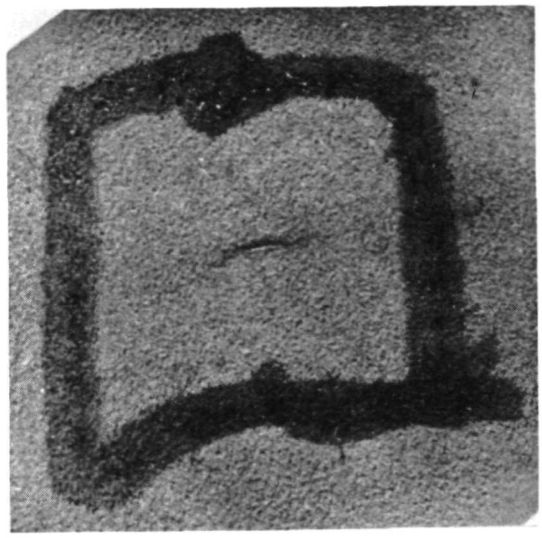

Figure 7A,DR-126. Small crack in side wall of shield ~ 1/4" long, 4" below top weld at 270°.

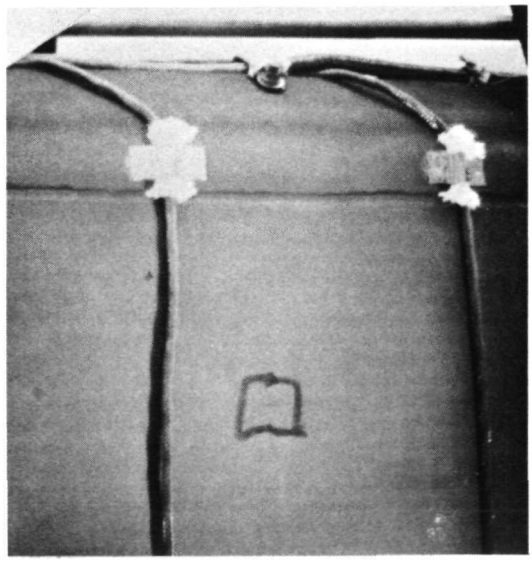

Figure 7B,DR-127. Low power Kollmorgen shot showing orientation of small crack.

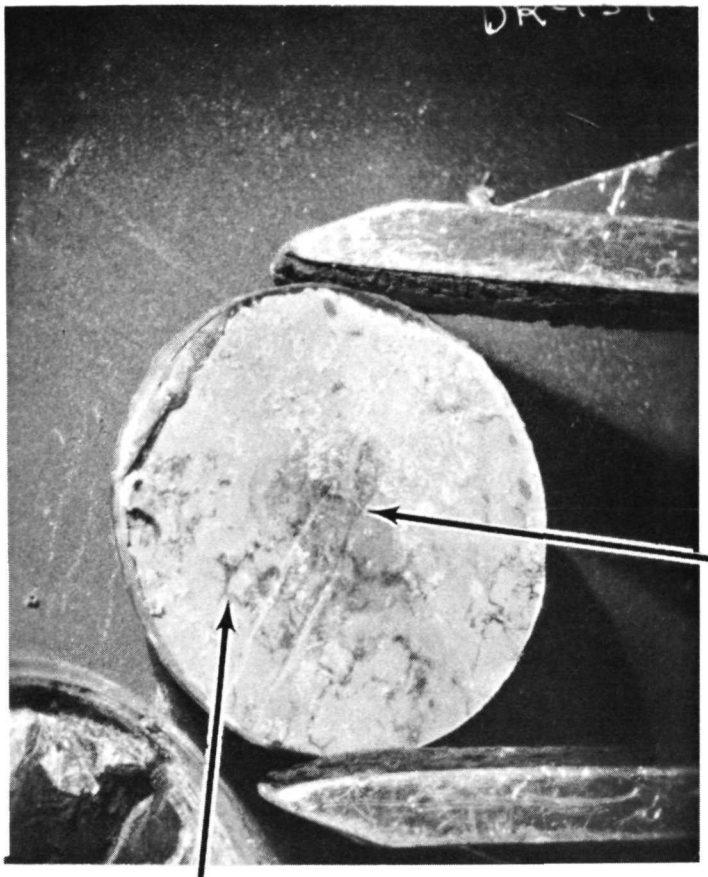

Figure 8, DR-134. Stainless Steel Wafer - Back side showing weld bead - main crack is centrally located (1.3X)

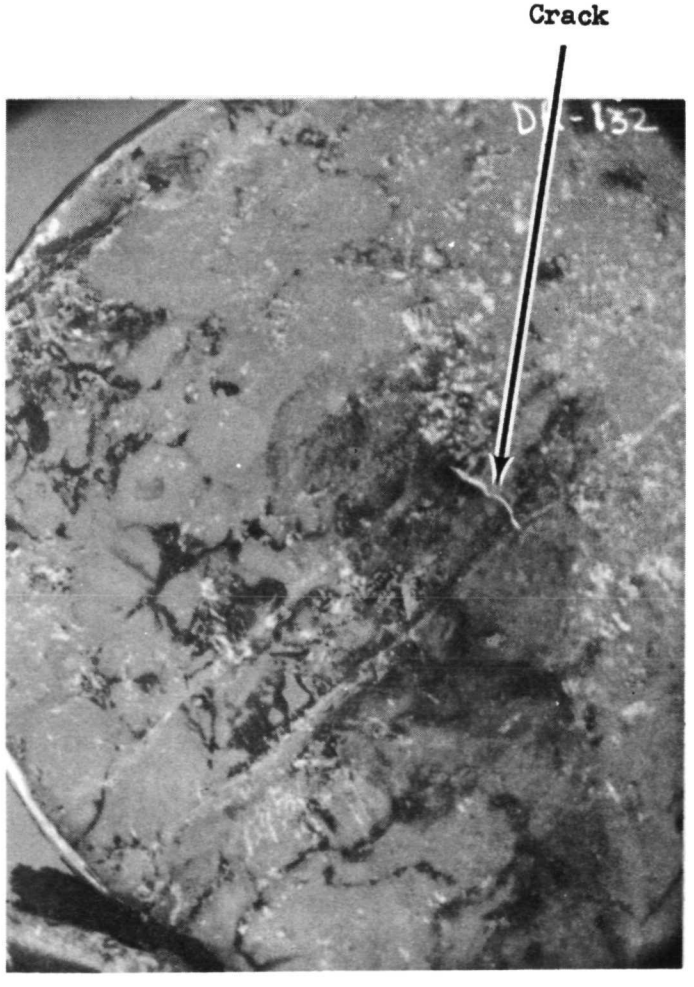

Figure 9, DR-132. Closeup (3.4X) of Main Crack in Weld Bead

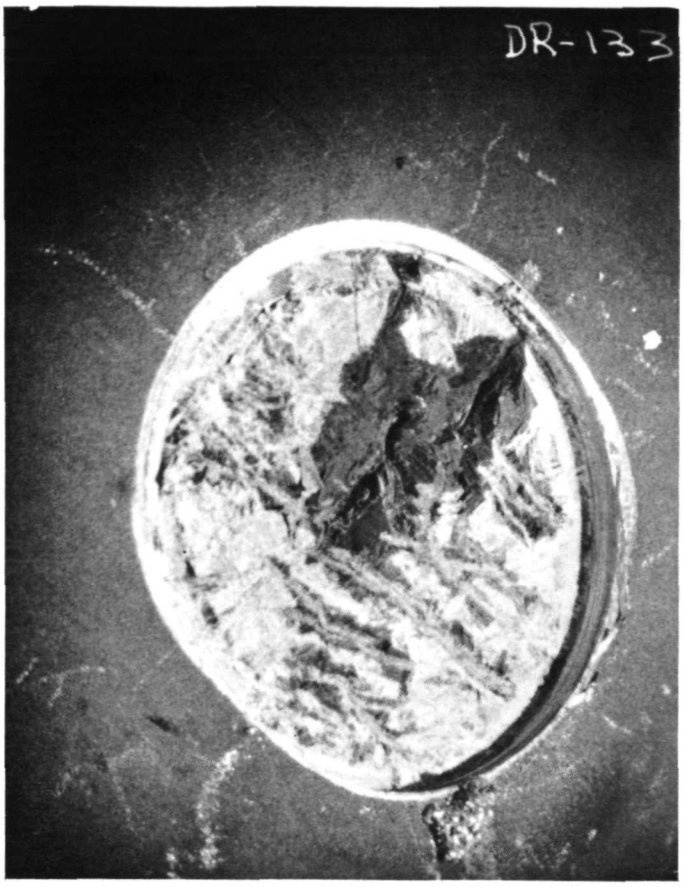

Figure 10, DR-133. Typical Crystalline Structure of Irradiated LiH (1.4X)

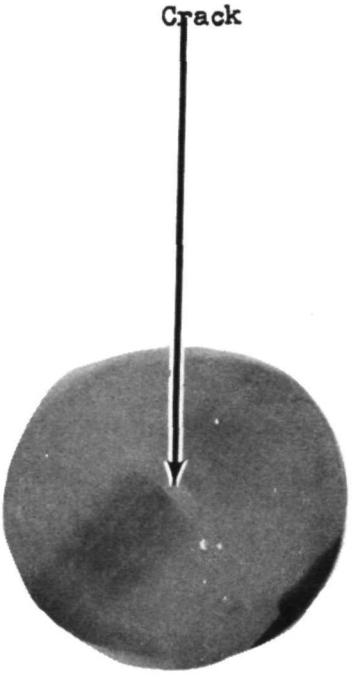

Figure 11, DR-151 X-ray. X-ray Showing Crack (taken perpendicular to face of wafer)

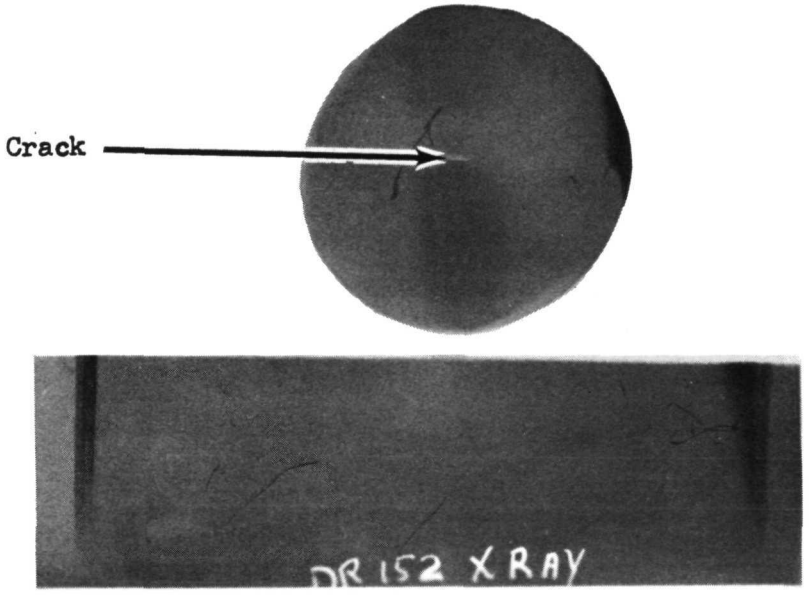

Figure 12, DR-152 X-ray. X-ray Taken 45 Degrees to Face of Wafer

Figure 13, DR-141. Photograph of Main Crack - Inside Surface (12.8X)

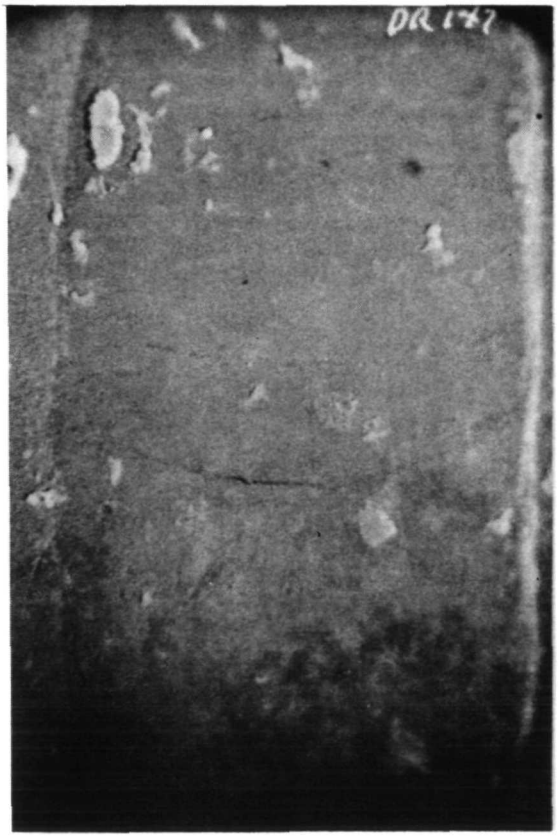

Figure 14, DR-147. Photograph of Hairline Crack Located ~ 1/2 inch From Main Crack (12.8X)

Figure 15, DR-142. Photograph of Three Small Cracks Located ~ 1/4 Inch from Main Crack (12.8X)

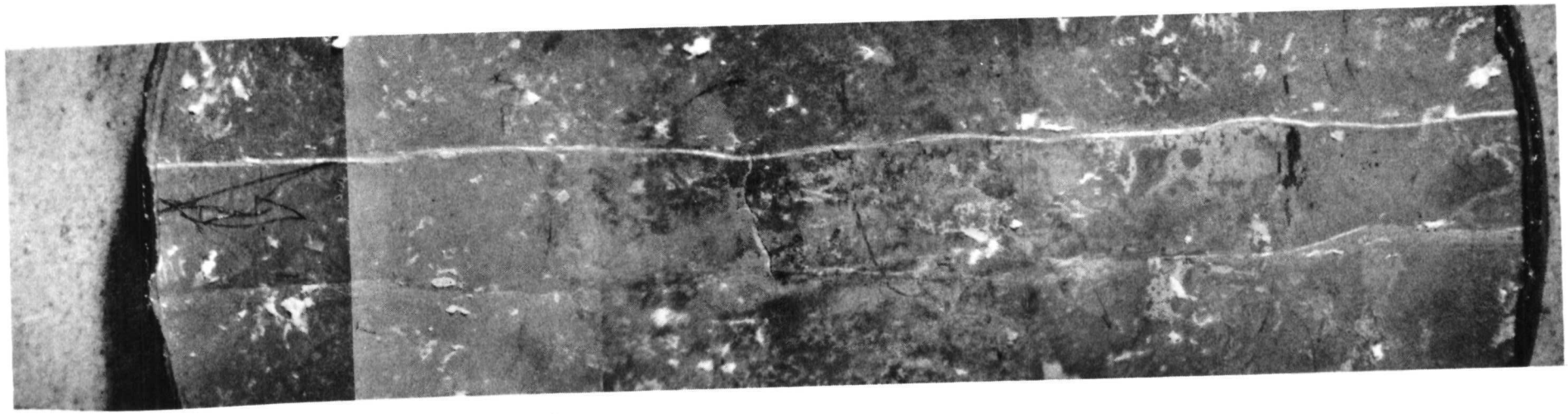

Figure 16. Stereo Photograph of Weld Showing Cracks (12.8X)

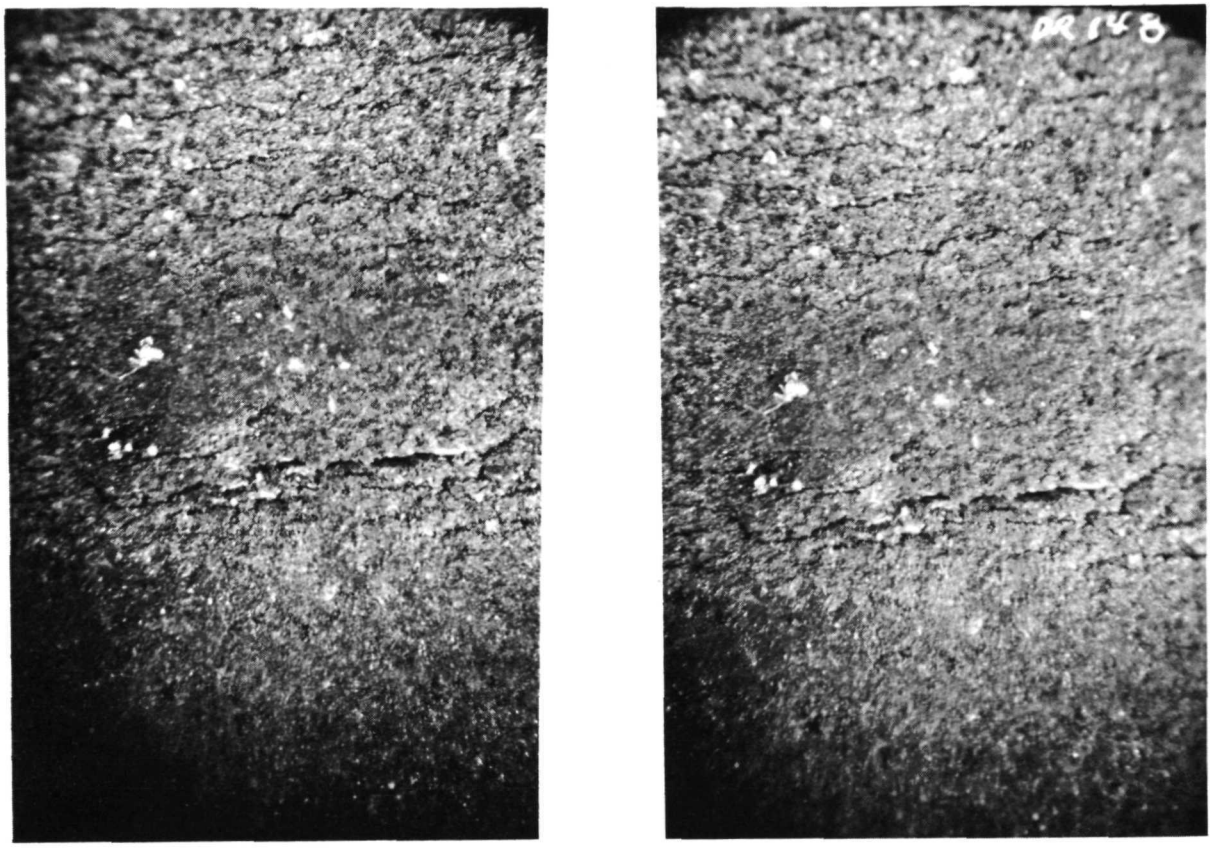

Figure 17, DR-148. Stereo Photograph of Outside Surface Showing Main Crack and Other Surface Cracks Not Related to Other Metal Cracks (12.8X)

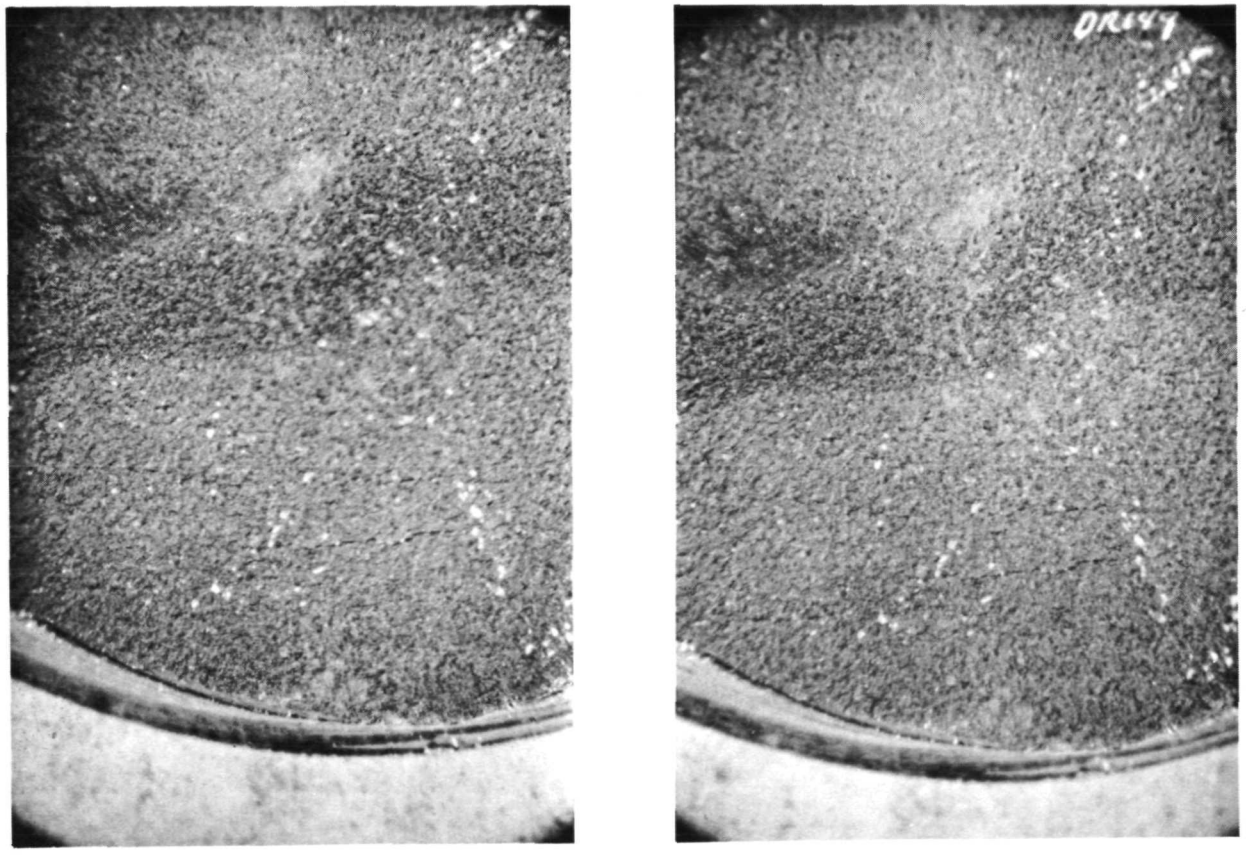

Figure 18, DR-149. Stereo Photograph of Outside Surface Showing Emissivity Coating Cracks Not Related to Metal Cracks (4.3X)

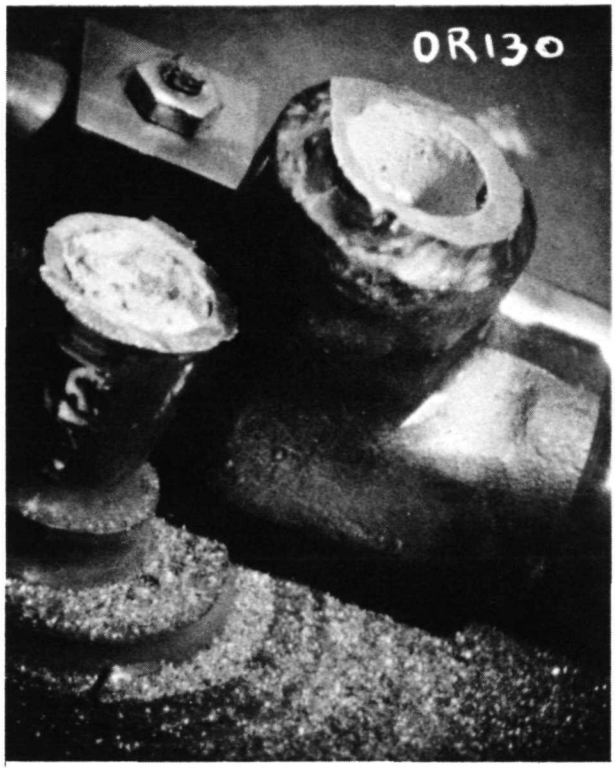

Figure 19, DR-130. Pipe Elbow Showing Lithium Hydroxide in Pipe Nipple

Figure 20, DR-140. View of Wafer Cut Out of Top Head Showing Inside Surface (1.4X)

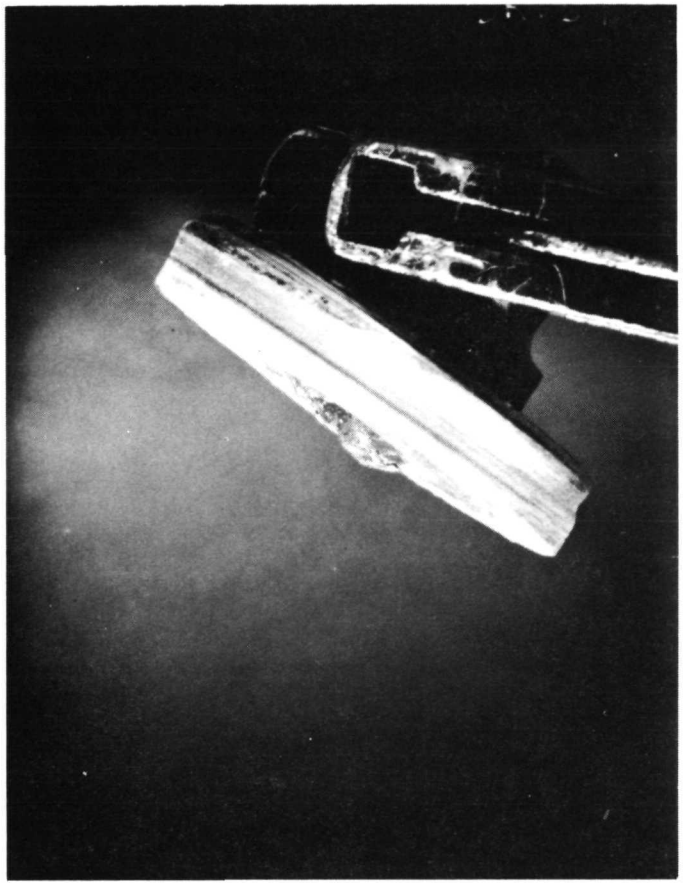

Figure 21, DR-139. View of Wafer Cut From Center of Head Showing LiH Crystalline Structure at Shield End of Pipe Nipple (1.4X)

Figure 22, DR-136. View of Wafer and Hole at Shield Head Mid-radius

Atomics International
North American Rockwell

SUPPORTING DOCUMENT

NUMBER	REV LTR/CHG NO.
TR-568-230-002	SEE SUMMARY OF CHG

PROGRAM TITLE
S8 DR Shield Examination

DOCUMENT TYPE
Test Report

KEY NOUNS
347 Weld Crack Investigation

DOCUMENT TITLE
Investigation of a Weld Crack in a Type 347 Stainless Steel Shield Assembly, P/N S8DS-13003

ORIGINAL ISSUE DATE
January 16, 1973

GO NO.	S/A NO.	PAGE 1 OF TOTAL PAGES 14
08306	10000	REL. DATE 1-18-73

PREPARED BY/DATE — DEPT — MAIL ADDR
R. E. Fish RE Fish — 737-732 — LB32

IR&D PROGRAM? YES ☐ NO ☐ IF YES, ENTER TPA NO. _____

APPROVALS — DATE
J. P. Page John P. Page 1-17-73

SECURITY CLASSIFICATION

(CHECK ONE BOX ONLY)	AEC	DOD
UNCL	☐	☒
CONF.	☐	☐
SECRET	☐	☐

(CHECK ONE BOX ONLY)
RESTRICTED DATA ☐
DEFENSE INFO. ☐

AUTHORIZED CLASSIFIER — DATE

DISTRIBUTION

*	NAME	MAIL ADDR

ABSTRACT

This report describes an investigation of a crack in a type 347 stainless steel weld observed approximately seven years after fabrication. Based on metallographic examination it was concluded that the crack emanated from a weld fissure or similar weakness which was induced but not detected during original fabrication. Initiation and propagation of the discontinuity into a detectable leak path was probably due to operational stresses. Such fissures are not uncommon to type 347 stainless steel and can be prevented by adding weld filler metal containing small amounts of delta ferrite.

RESERVED FOR NR PROPRIETARY/LEGAL NOTICES

* TITLE PAGE ONLY

FORM 734-C REV 4-71

Page Intentionally Left Blank

INTRODUCTION

A crack was visually observed in the longitudinal seal weld of the cone portion, P/N S8DS-13004-3, of a shield assembly, P/N S8DS-13003. The crack extended transversely across the weld fusion zone and slightly into the heat affected zones on both sides of the fusion zone (f igure 1). The crack extended through the thickness of the weld.

The assembly was fabricated circa 1965. The weld was made using the gas tungsten arc process (GTAW) in 0. 109 inch thick Type 347 stainless steel procured to specification MIL-S-6721. The weld symbol denoted a full penetration weld using a straight-butt (no groove) preparation. After welding, the fusion zone was made flush by roll planishing. Following this operation the weld was examined using liquid penetrant, radiographic, and helium mass spectrographic methods. Although a record search was not conducted, there is no reason to doubt that all the operations were completed satisfactorily and that the weld was acceptable.

The assembly experienced the following thermal excursion:

1450F for 2-3 days, cool at 30°F to 1050°F
1050F for 2 days
Operation at 400°F.

TEST PROCEDURE AND RESULTS

A portion of the weld containing the crack was trepanned from the shield. Plastic replicas were made of this section. It was noted that the I. D. (root side) had not been made fully flush by the roll planishing operation as evidenced by .005-.010" protrusion of residual drop through (figure 2).

The section was mounted such that the face surface (figure 2) was accessible for polishing. This surface was prepared metallographically for analysis of the microstructure.

Examination of the metallographic mount showed that the crack was intergranular and appeared to initiate at a small discontinuity at the approximate center of the weld (figures 3 and 4). It was also noted that the dendritic structure was distorted, apparently a result of planishing, and did not follow

a normal semi-circular or triangular freezing pattern (figures 1 and 3). There were islands of what initially appeared as equiaxed grain structure observed in the fusion zone (figures 1, 3, and 4). This was considered abnormal for the weld involved and was later interpreted as recrystallized cold-worked material (see discussion). The structure was essentially all-austenitic with virtually no delta ferrite visible (figure 4). This conclusion was reached by comparing the viewed structures with weld structures known to contain specific delta ferrite contents.[4] The dendritic formations (other than being distorted) were generally long, narrow, and almost perpendicular to the direction of rolling (figures 1 and 3). There was no evidence of sigma phase.

DISCUSSION

It is a virtual certainty that the crack propagated from an undisclosed defect, most probably a micro-fissure occurring during the original longitudinal GTA welding of the conical section. This conclusion is based on the well-known propensity of type 347 stainless steel for hot short cracking[1, 2] in conjunction with the known limitations of the non-destructive examination methods which were applied to the weld.

The element columbium, Cb (Niobium, Nb) is added to type 347 stainless steel to prevent chromium depletion due to chromium carbide formation and precipitation, at grain boundaries, during periods of exposure to elevated temperatures, e.g., welding. This depletion reduces the corrosion resistance of the alloy (sensitization). Carbon preferentially combines with the columbium additive, thus preventing removal of chromium from the system (stabilization). However, surplus columbium combines with iron, Fe, to form a low melting constituent (Fe, Cb). This constituent, under unfavorable weld solidification conditions and being molten as a grain boundary film during high applied shrinkage stress, results in void discontinuities ranging from micro-fissures to macro-cracks. It is logical and highly probable that the fissure which occurred in the shield weld did not originally extend to either face; hence escaping detection by both liquid penetrant and helium mass spectrographic examinations. It is equally likely that the fissure was spatially oriented to elude disclosure by radiographic examination. Some amount above 10° out-of parallelity with the direction of radiation would accomplish this.

Progression of the fissure probably occurred during the thermal cycling operations, but apparently not to the extent of providing a through-leak path. This latter event obviously occurred due to whatever loading the weld experienced in service.

As previously mentioned, hot fissuring in type 347 stainless steel has not been an unusual experience. This same experience naturally generated many extensive studies to derive the causes and means of reducing similar problems in any austenitic weld deposit. The results of these studies[2, 3] recognized that controlling the composition of the filler metal to result in a weld deposit containing 3% to 10% delta ferrite effectively reduced or eliminated hot fissuring in all-austenitic welds. The filler wire manufacturers responded appropriately and it has been practice to provide 300 series stainless steel filler wires with not less than 5% ferrite potential since the early 1960's, even though it was not required by government or society procurement specifications until late 1972 (ASME Code).

A review of the metallographic evidence of this investigation shows that the conditions involved in making the weld in fact promoted the formation of the offending fissure:

a. The presence of major amounts of dendritic structure (although distorted), minor amounts of recrystallized cold worked structure, and residual physical drop-through are all strong indicators that the material movement due to the roll planishing required to flush the weld face surface was very small.

   (Roll planishing is an operation in which a weld bead is passed between two rolls under sufficiently high pressure to cause the material to yield and conform to the thickness and contour of the adjacent parent metal. It is applied to remove the effects of weld-induced distortion due to shrinkage where dimensional control is important, to refine the as-welded nugget cast structure by cold work and subsequent recrystallization where mechanical properties more similar to wrought material are important, and/or to flush the weld surface for fit or cosmetic purposes. Metallographically, the cold-worked and recrystallized structure will exhibit very little prior dendritic structure.)

b. The perpendicularity of the dendritic structure disclosed that a welding procedure had been used which was conducive to weld fissuring. Continuing research programs at Rensselaer Polytechnic Institute, Troy, N.Y. by Dr. Warren Savage, et al.[5, 6, 7], have shown that weld puddle shape definitely controls the directionality of dendrite grain epitaxial growth. A triangular pattern, or tear drop puddle, results in the perpendicular direction observed in the shield weld (figure 5A). A semi-circular pattern, or elliptical puddle, results in a more variable curving direction (figure 5B). Solidification direction should not be confused with the mechanical ripple pattern which appears on an as-welded bead (figure 5). Ripple is caused by a complex interaction of solid/liquid interface progression and varying surface tension (amended by mechanical agitations in weld velocity or filler wire feed)[8]. Savage's work[9] also concluded that a perpendicular pattern generated conditions more susceptible to center-bead cracking in alloys unforgiving of such conditions (such as 347). The tear-drop puddle forces final freezing of large amounts of segregate (in this case Fe, Cb) to occur at the weld center-line. The elliptical puddle distributes the segregate in smaller amounts over a longer path, thus reducing fissuring incidence. The teardrop shape is associated with high welding speed.

(Note: It was partly for this reason that the non-dendritic islands in the metallographic section were interpreted as being grains refined by cold work and recrystallization, rather than equiaxed grains. The latter are affected by relatively long solidification times under stagnant conditions.)

c. The virtual total absence of ferrite in the weld fusion zone was indicative that very little weld filler was added during welding. More probably, none was added. This is not unusual practice when post-weld planishing is to be performed. An autogenous (fillerless) GTA weld, made using a suitable stake fixture,

conventionally utilizes a grooved backing mandrel--usually copper (figure 6A). The molten nugget is literally "cast" into this groove deliberately to result in minimal drop-through of uniform dimensions and a weld face exhibiting some amount of uniform concavity (figure 6B). This cross-section may be much easier to planish flat, but may not achieve the objectives for planishing mentioned earlier.

Since the role of delta ferrite is no less important in an autogenous weld, base metal with a ferrite potential less than 3% is expected to fissure or crack in such a weld. It is safe to assume that most product forms of austenitic stainless steels bear minimum ferrite. In rolling, drawing, extruding, etc. operations, ferrite is a real structural discontinuity which frequently results in tears, splits, and seams which can scrap an entire heat of metal. Naturally, the metal producers will refrain from working heats known to contain ferrite. It is normal good practice in the welding industry not to weld types 347 and 316 stainless steels autogenously unless the composition is such that a minimum of 3% delta ferrite in the fusion zone is probable, and/or a suitable weldability test has been performed.

CONCLUSIONS

The following sequence of events occurred:

1. A low ferrite level heat of material was autogenously GTA-welded at high speed, resulting in an internal micro-fissure.
2. A moderate amount of cold work was imparted to the weld by roll planishing (figure 4C).
3. The fissure was not propagated sufficiently, if at all, to be detected by liquid penetrant, helium mass spectragraphic and radiographic examinations.
4. The weld was subjected to thermal excursions which recrystallized the cold worked portions of the weld and probably propagated the fissure (crack) to just short of resulting in leakage.

5. Loads imposed on the weld in service propagated the crack to final failure.
6. Grinding away the outer surface of the weld section during metallographic preparation removed most of the recrystallized structure and exposed the dendritic structure (figure 5C).

RECOMMENDATION

Welding of type 347 (or type 316) stainless steel without adequate addition of weld filler metal of a composition which can yield at least 3% delta ferrite must be prohibited in applications where weld fissuring or cracking is intolerable. Exceptions can be made if the composition of the base metal meets the 3% ferrite level, or a suitable weldability test has been performed and the material judged to be weldable.

REFERENCES

1. Welding Journal, December 1966, pp 539s and 560s, "Stainless Steel; Stabilized--Technical Note," C. R. Sibley.

2. Defects and Failures in Pressure Vessels and Piping, Helmut Thielsch, Reinhold Publishing Corp., 1965.

3. Welding Journal, September 1967, pp 399s-409s, "Effect of Delta Ferrite on the Hot Cracking of Stainless Steel," F. C. Hull.

4. Preparation, Characterization, and Testing of Austenitic Stainless Steel Weldments, HEDL Report No. HEDL-TME 71-118, August, 1971; A. L. Ward, et al.

5. Welding Journal, February 1966, pp 85s-89s, "Preferred Orientation in the Weld Fusion Zone," W. F. Savage and A. H. Aronson

6. Welding Journal, November, 1968, pp 522s-528s, "Solidification of Fusion Welds in Face Centered Cubic Material," W. F. Savage, C. D. Lundin, and T. F. Chase.

7. Welding Journal, May, 1972, pp 260s-271s, "Synthesis of Weld Solidification Using Crystalline Organic Materials," W. F. Savage and Robert J. Hrubec.

8. Welding Journal, February 1970, pp 41s-45s, "Sources and Effects of Growth Rate Fluctuations During Weld Metal Solidification," A. T. D'Annessa

9. Welding Journal, September 1968, pp 420s-425s, "Segregation and Hot Cracking in Low-Alloy Quench and Tempered Steels," W. F. Savage, C. D. Lundin, and R. J. Hrubec.

Figure 1. Macrophotographic Montage Showing Relationship of Crack and Weld Zones

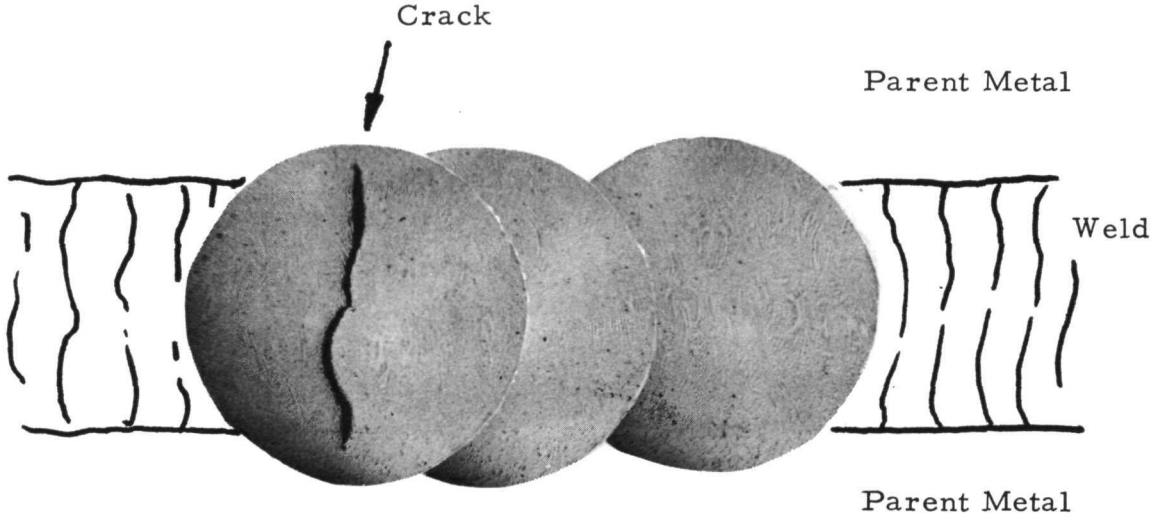

Mag: Approx. 8X Etchant: Aqua Regia

View looking down at outer surface of weld (top surface removed by metallographic preparation). Note distortion of dendritic structure caused by roll planishing. Also note areas of recrystallized structure (lighter appearance) caused by roll planishing and subsequent exposure to elevated temperature.

Figure 2

Cross-Sectional Illustration of
Weld Finishing Operations by Roll Planishing

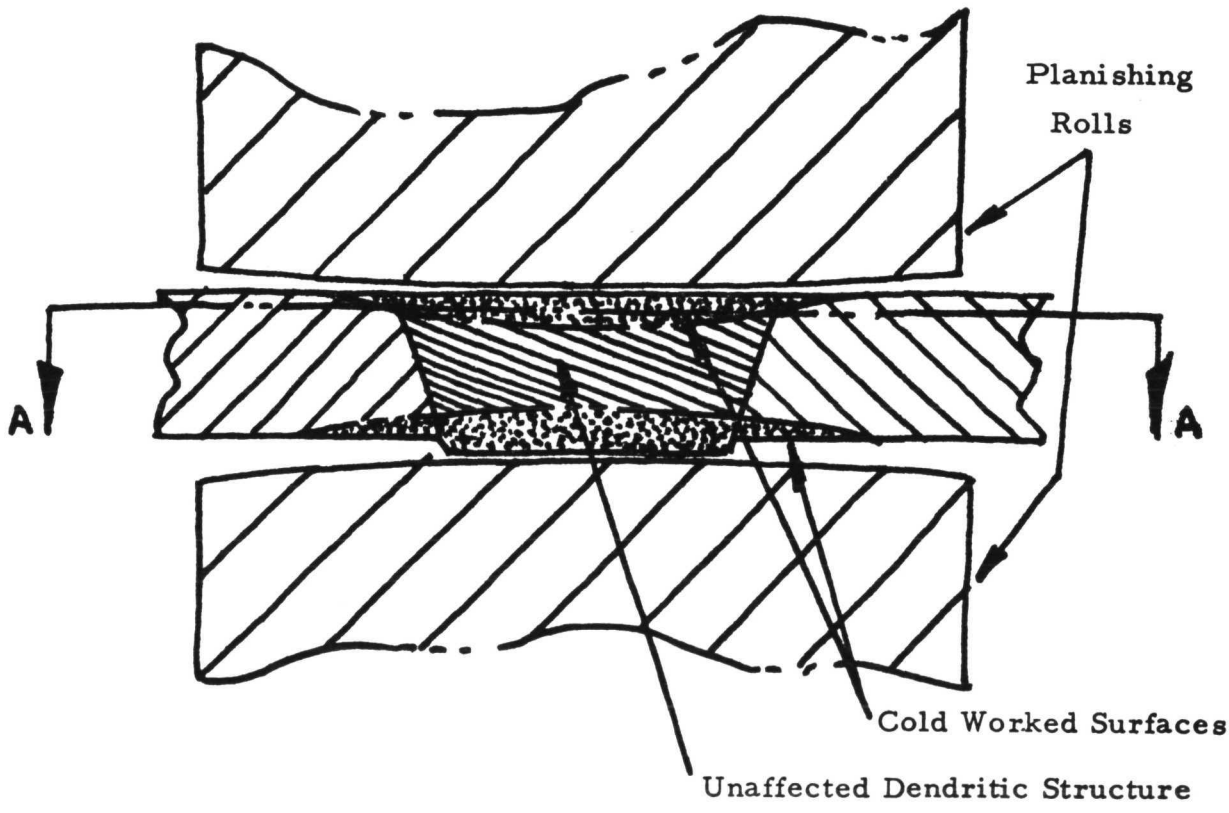

A-A represents top view metallographic mount shown in Figure 1.

Figure 3

Enlargement of Same View Shown in Figure 1

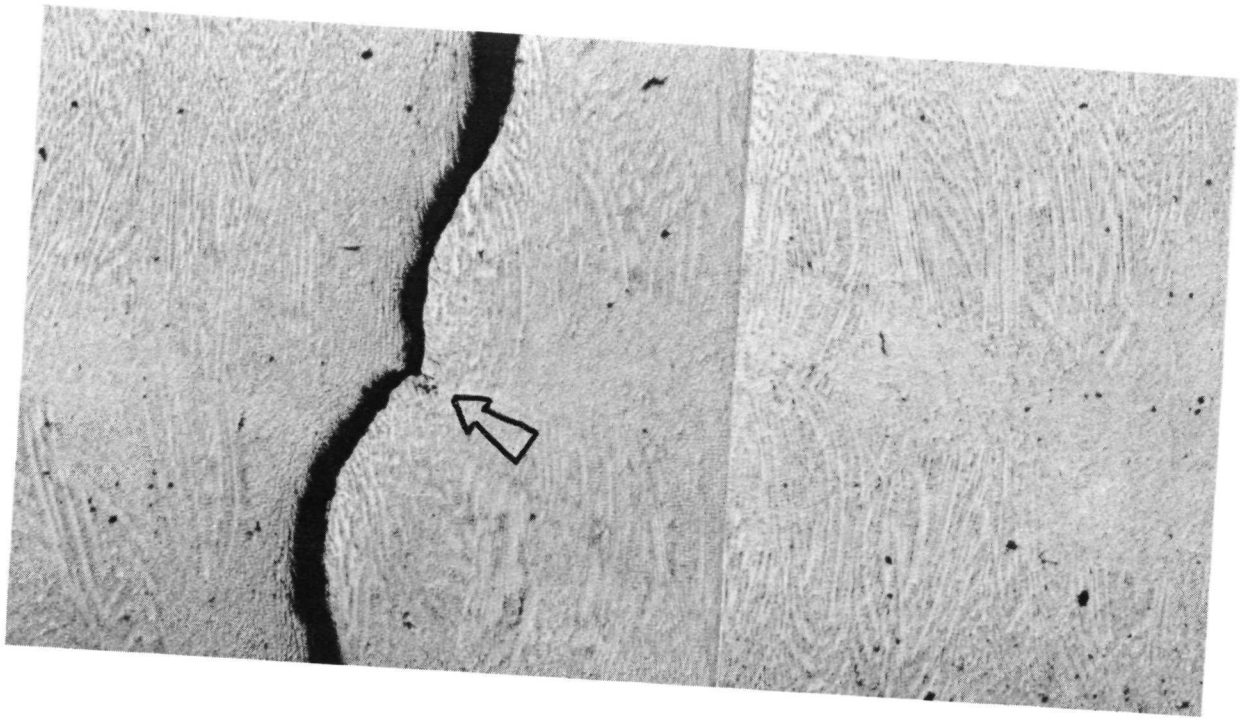

Mag: Approx. 30X

Etchant: Aqua Regia

Arrow denotes possible initiation point of crack at a clustered discontinuity. Distorted dendritic structure and recrystallized zones are obvious. Propagation appears to be intergranular.

Figure 4

Enlargement of Point of Possible Crack
Initiation Denoted in Figure 2

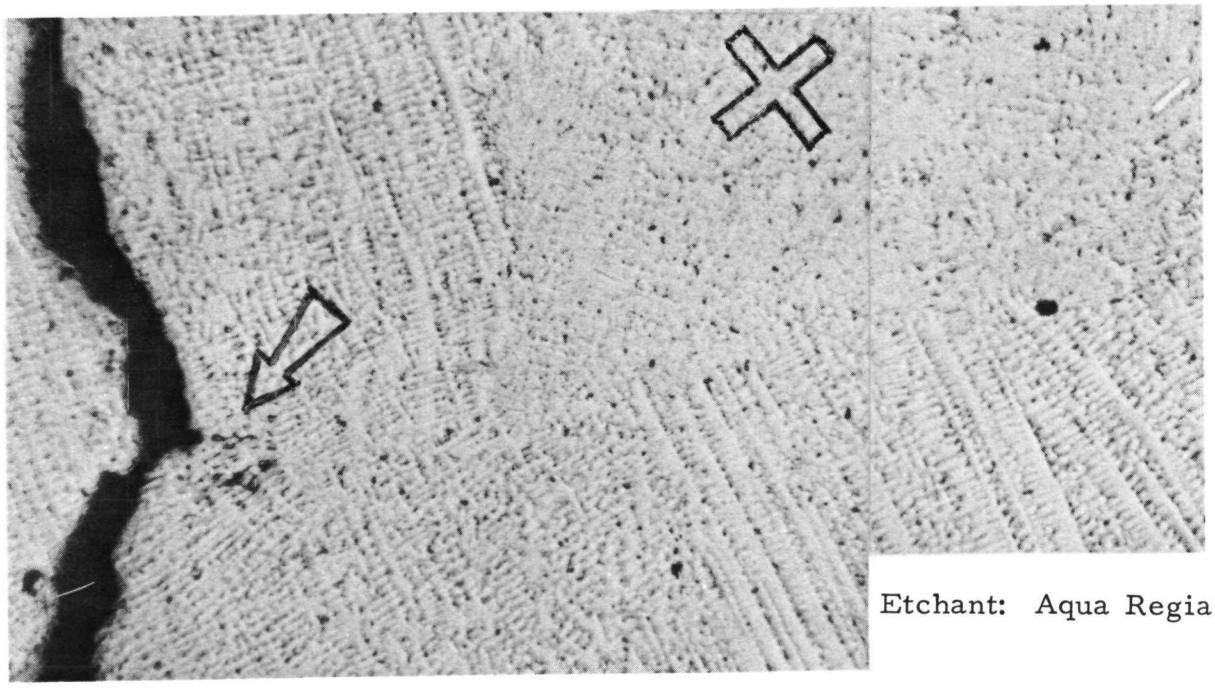

Etchant: Aqua Regia

Mag: 100X

Discontinuity cluster is obvious (arrow). Cross denotes recrystallized structure. Note that some residual dendritic structure is still evident in this zone, implying that cold work due to planishing was only modest. Also note virtual absence of delta ferrite (dark etching interdendritic constituent).

Figure 5

Illustrations of Weld Puddle Solidification Modes
(Viewed Looking Down at Weld Face Surface)

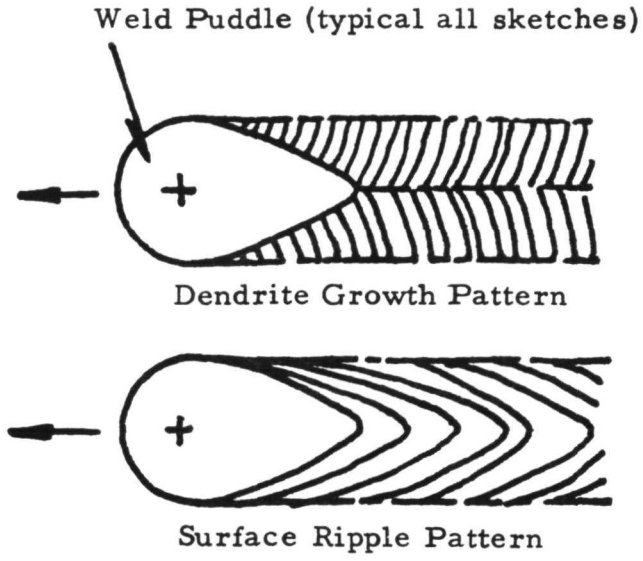

A. Triangular Pattern. The tear drop shape is associated with high speed, center-bead segregation, and center-bead cracking. This was typical of the weld examined in this investigation.

B. Semicircular Pattern. The elliptical shape is associated with lower speed, reduced localized segregation, and reduced fissuring in hot short alloys.

Figure 6

Cross-Section Illustrations of
Weld Fabrication Progression

A. Probable Weld Joint Preparation

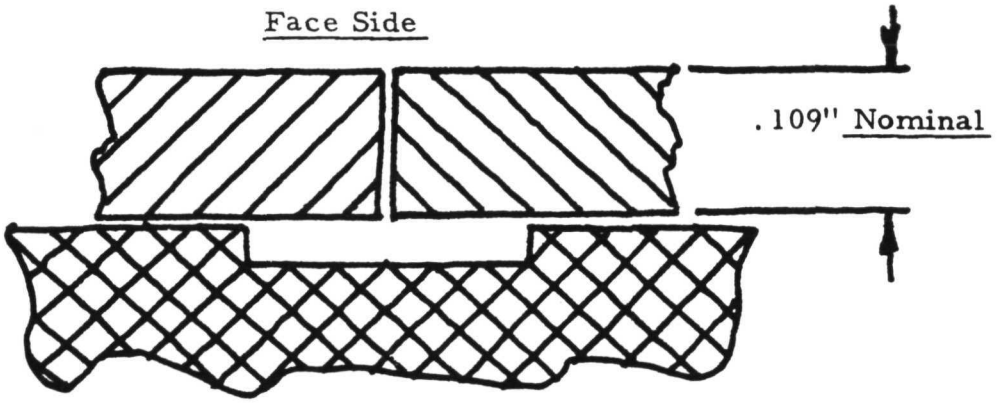

B. Probable As-Welded Fusion Zone Geometry

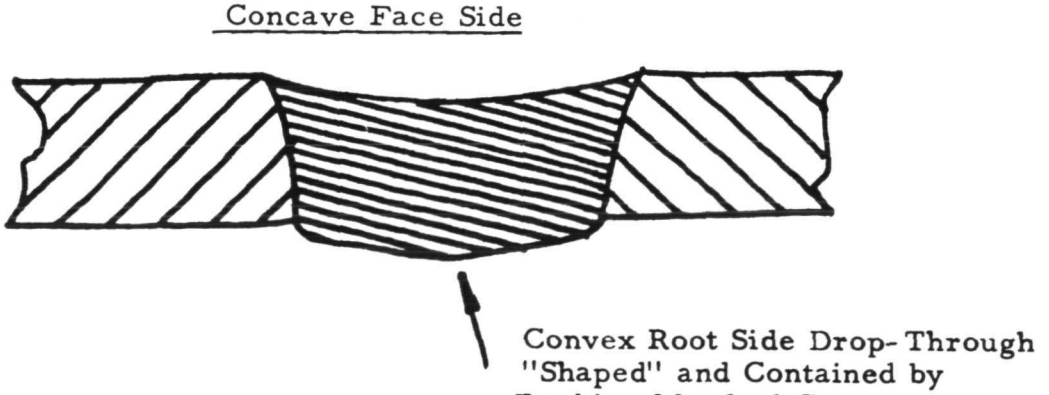

DISTRIBUTION

Argonne National Laboratory
9700 South Cass Avenue
Argonne, IL 60440
Attn: E. N. Pettitt

Atomic Energy Commission
Washington, D.C. 20545
Attn: Hdqtrs. Library, Reports Section, MS G-017
Donald S. Beard
Ronald Anderson
C. McCallum

Atomic Energy of Canade Limited
Whiteshell Nuclear Research Establishment
Chemistry and Materials Science Division
Pinawa, Manitoba, Canada
Attn: R. F. Robertson, Division Director

Bettelle Memorial Institute
505 King Avenue
Columbus, OH 43201
Attn: W. Chubb
H. Russell

Donald W. Douglas, Inc.
2955 George Washington Way
Richland WA 99352
Attn: Correspondence Control

General Electric Co.
Nuclear Systems Program
P.O. Box 15132
Cincinnati, OH 45215
Attn: H. C. Brassfield

General Electric Co.
Nuclear Thermionic Power Operation
P. O. Box 846
Pleasanton, CA 94566
Attn: J. Danko

General Electric Co.
Nuclear Energy Division (MC-328)
P.O. Box 1131
San Jose, CA 95108
Attn: Alleen Thompson

Gulf Energy & Environmental Systems
P.O. Box 608
San Diego, CA 92112
Attn: L. Perry

Hittmann Associates, Inc.
Route 108
Columbia, MD 21043
Attn: H. Hagler

Jet Propulsion Laboratory
4800 Oak Grove Drive
Pasadena, CA 91103
Attn: J. F. Mondt

Los Alamos Scientific Laboratory
P.O. Box 1663
Los Alamos, NM 87544
Attn: Report Librarian, W. Reichelt

NASA Headquarters
Washington, D.C. 20546
Attn: RPE/J. Lazar
NS-1/P. Miller
NS-2/D. Gabriel

NASA Scientific and Technical Information Facility
Box 33
College Park, MD 20740
Attn: NASA Representative (10)

NASA Manned Spacecraft Center
Houston, TX 77058
Attn: Librarian

Oak Ridge National Laboratory
Oak Ridge, TN 37830
Attn: A. Fraas
J. L. Scott
C. E. Clifford

Westinghouse Electric Corporation
Westinghouse Astronuclear Laboratory
P. O. Box 10864
Pittsburgh, PA 15236
Attn: J. G. Gallagher

2 of 2

Westinghouse Electric Corporation
Bettis Atomic Power Laboratory
West Mifflin, PA 15122
Attn: H. R. Warner

NASA Lewis Research Center
21000 Brookpark Road
Cleveland, OH 44135

Attn:	Lewis Library (2)	MS 60-3
	Report Control Office	MS 5-5
	G. M. Ault	MS 3-5
	R. E. English	MS 500-201
	L. J. Kaszubinski (4)	MS 49-3
	S. J. Kaufman	MS 49-2
	M. H. Krasner	MS 49-3
	N. T. Musial	MS 500-311
	H. L. Staubs	MS 501-3
	L. W. Schopen	MS 500-206
	R. P. Migra	MS 49-3